Upper mantle velocity structure beneath the Korean Peninsula by teleseismic traveltime tomography: evidence for heterogeneous modification and reactivation of a cratonic lithosphere margin

T13E-0236

Jung-Hun Song[1](wjdgns230@snu.ac.kr), Seongryong Kim[2], Junkee Rhie[1]

[1]School of Earth and Environmental Sciences, Seoul National University, Seoul, Korea, [2]Department of Geological Sciences, Chungnam National University, Daejeon, Korea

서울대학교 SEOUL NATIONAL UNIVERSITY

Abstract

Margins of old continental lithosphere are likely prone to ongoing modification processes. Therefore, constraining detailed structures beneath the margin can be essential in understanding the evolution of the continental lithosphere. . The eastern margin of the Eurasian plate is a natural laboratory that allows us to study the strong effects from multiple episodes of continental collision and subduction of different oceanic plates since their formation. To reveal the detailed evolution of cratons at their margins, we describe, for the first time in detail, 3-D upper mantle velocity structure beneath the southern Korean Peninsula (SKP) by teleseismic traveltime tomography. We used seismic data recorded by 254 permanent stations deployed in and around SKP, which allowed us to obtain high-resolution P and S wave velocity structures from the uppermost mantle to a depth of ~360 km. We found a prominent velocity contrast within the peninsula showing relatively low velocity in the east and northeast while relatively high velocity in the west and southwest. We imaged a thick (~150 km) high-velocity anomaly mainly beneath the Proterozoic Yeongnam massif with large velocity contrasts (*dlnVp* ≈ 4.0% and *dlnVs* ≈ 6.0%) at its boundaries, suggesting the presence of a long-lasting cratonic root in the southwestern SKP. On the other hand, low-velocity anomalies were found beneath the Proterozoic Gyeonggi Massif, Gyeongsang arc-back-arc basin, and along the eastern margin of the SKP, indicating significantly modified regions. The possible existence of a remnant cratonic root beneath the SKP and contrasting lithospheric structures across the different Precambrian massifs suggests the highly heterogeneous modification of cratonic lithosphere at the eastern Eurasian plate margin. Strong velocity reductions, which indicate a thermally elevated upper mantle with potential partial melts, clearly correspond to areas of Cenozoic basalts, high surface heat flow, and high topography along the eastern KP margin. We interpret this coincidence as a result of recent reactivation of a craton margin, which is controlled by intense interaction between the convective upper mantle and heterogeneous continental lithosphere.

Data & Methods

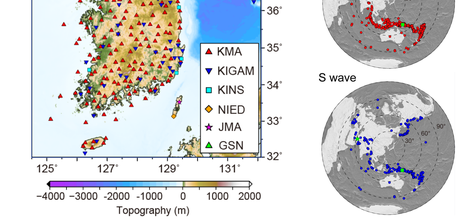

Seismic stations & events

We used teleseismic body wave (direct *P*, *S*) to measure relative arrival time residuals. The seismic stations consist of accelerometers, short-period, and broadband stations operated by Korea Meteorological Administration (KMA), Korea Institute of Geoscience and Mineral Resources (KIGAM), Korea Institute of Nuclear Safety (KINS), Japan Meteorological Agency (JMA), F-net of National Research Institute for Earth Science and Disaster Resilience (NIED), and Global Seismic Network (GSN) (left, Fig. a). Locations of stations and events are shown in the left. We selected teleseismic events occurred between 2013 to 2018 with magnitudes larger than mb 5.4 in epicentral distances 30°–95°. Total 684 and 274 sources were used for P and S wave arrivals, respectively (left, Fig. b).

Relative traveltime measurement & Data inversion

Relative arrival time residuals were accurately measured using the adaptive stacking method (Rawlinson et al., 2004). Examples of waveforms and calculated relative residuals are shown below. We observed *P* and *S* waveforms in a vertical component with bandpass filtered between 0.1-5.0 Hz and in a transverse component with bandpass filtered between 0.1-1.0 Hz, respectively. We applied Fast Marching Tomography (FMTOMO, Rawlinson & Urvoy, 2006) to invert residual dataset to 3-D velocity perturbations. The method applies Fast Marching method (FMM, Rawlinson & Sambridge, 2004), which is a grid-based eikonal solver for calculating wave propagation in a 3-D local model space, and a subspace inversion technique (Kennett et al., 1988) for an inversion. Forward traveltime prediction and inversion procedures were iteratively applied to solve a non-linear tomography inversion. To account for crustal effects, we simultaneously inverted the model for crustal and upper mantle structures with fixed Moho depths. Instead of using local crustal models in the SKP, a global crustal model (Crust1.0; Laske et al., 2013) was adopted to cover regions beneath not only the SKP but also its margins and off-coasts.

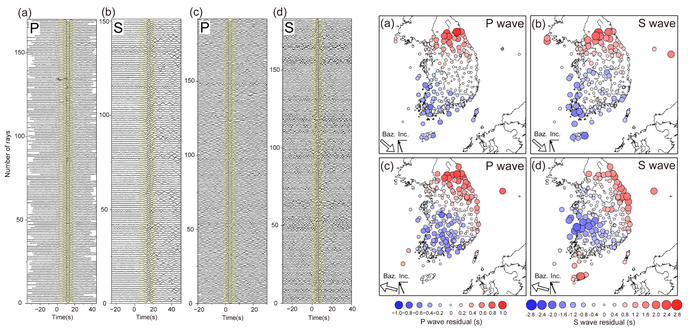

Residual correction for lower upper mantle heterogeneity

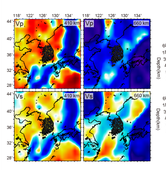

3-D lower upper mantle velocity model (Tao et al., 2018)

Although the effect of velocity heterogeneities outside the model space is less significant due to similar ray trajectories (Aki et al., 1977), strong velocity perturbations at relatively less-constrained bottom depths can potentially bias amplitudes and patterns of the estimated anomalies above. In our study area, regional tomography at depths of 400–800 km suggested velocity perturbations of up to 5% in the Vp and 7% in the Vs, mainly due to the stagnant Pacific slab in the mantle transition zone (Li and van der Hilst, 2010; Tao et al., 2018). We tested and minimized the impacts that the deeper anomalies had on our results. We first calculated synthetic residuals from a recent 3-D upper mantle velocity model for deeper depths (Tao et al., 2018) (left) and compared them with our observations. As a result, a long-period pattern of similarity was observed as a function of the back-azimuth between the observed and synthetic residuals (right), confirming that this pattern originates from deeper upper mantle structures. However, this effect caused only a small decrease in amplitude (dlnVp < 0.3% and dlnVs < 0.5%) in our images for shallower areas (< 300 km) based on an additional inversion with a corrected dataset generated by subtracting the synthetic data from the observations. As a conservative choice, we determined the results by inversion with the corrected dataset as our final model.

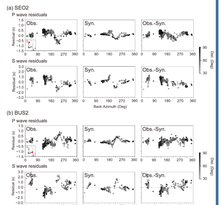

Tectonic setting

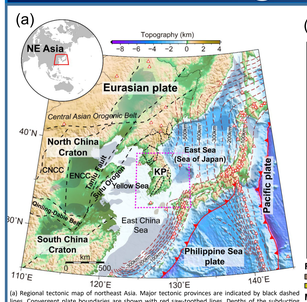

(a) Regional tectonic map of northeast Asia. Major tectonic provinces are indicated by black dashed lines. Convergent plate boundaries are shown with red saw-toothed lines. Depths of the subducting oceanic slabs are indicated by brown dashed contours at 100-km intervals. Cretaceous and Cenozoic extensional basins are shaded in gray. Volcanoes are indicated by red triangles. A pink dashed rectangular box shows the map boundary of Fig. 2. CNCC: central North China Craton; ENCC: eastern North China Craton; KP: Korean Peninsula. (b) Map showing the geology of the Korean Peninsula (KP). Black solid lines indicate the boundaries of the different geologic provinces. GB: Gyeongsang Basin; GM: Gyeonggi Massif; IB: Imjingang Belt; JI: Jeju volcanic Island; NM: Nangrim Massif; OB: Okcheon Belt; UI: Ulleung volcanic Island; YM: Yeongnam Massif.

The Korean Peninsula (KP) is located in the eastern margin of the Eurasian plate (Fig. a). The basement of the KP consists of late Archean to early Proterozoic massifs: from north to south, the Nangrim (NM), Gyeonggi (GM), and Yeongnam (YM) (Fig. b). As in China, each of the massifs in the KP were subject to different tectonic processes during amalgamations and breakups of supercontinents (Columbia, Rodinia, Gondwana, and Pangea) before the formation of the current setting since the late Paleozoic to early Triassic. Two fold-and-thrust belts, i.e., the Paleozoic Imjingang belt (IB) and late Precambrian-Paleozoic Okcheon belt (OB), separate the GM from the NM and YM, indicating collisional and accretional processes during their formation. Extensive Mesozoic-to-early Cenozoic plutonic emplacements followed in a post-collisional and subduction tectonic setting. Subsequent oblique subduction and rollback of the oceanic plates affected the Precambrian lithosphere from eastern China to the YM, forming the Gyeongsang arc-back-arc basin (GB) at the southeastern margin of the YM and rifted structures in the East Sea to the east of the KP, respectively. Spatially non-uniform and complex tectonic structures indicate that the cratonic lithosphere in the KP has been exposed to intensive, complicated modification processes at the continental margin during the Phanerozoic period (Chough et al., 2000).

Tomography Results

Horizontal cross-sections of Vp and Vs model

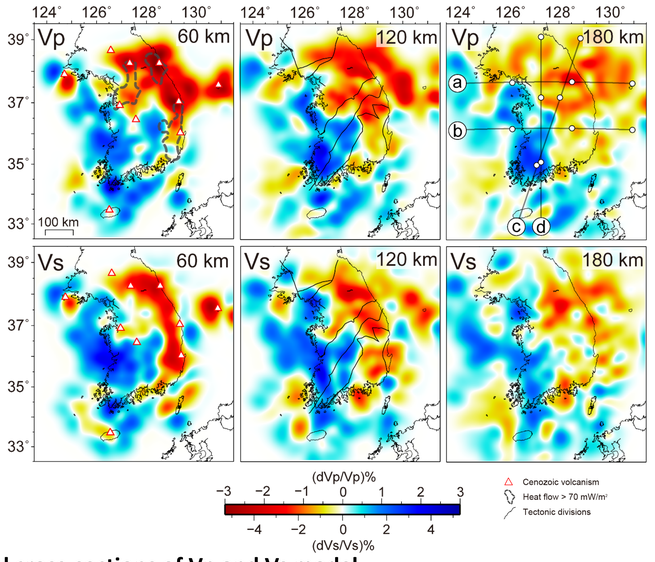

Vertical cross-sections of Vp and Vs model

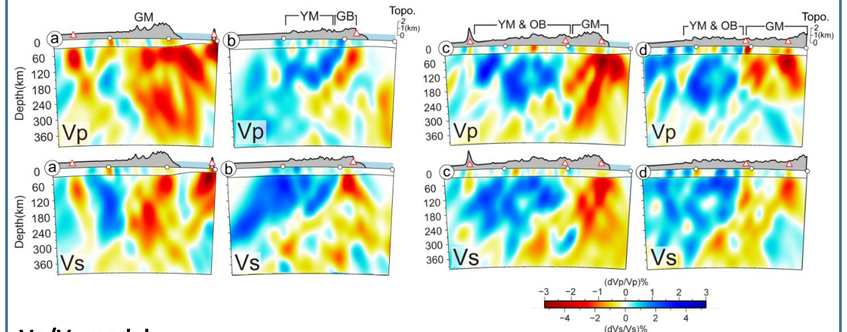

Vp/Vs model

We obtained a Vp/Vs model from a joint inversion of P and S wave residuals through the similar approach of Schmandt et al., 2010. We composed cost functions simply summing the individual cost functions of Vp and Vs and applying additional smoothing regularization for Vp/Vs perturbations by simultaneously modifing smoothing parameters of Vp and Vs based on the norm of Vp/Vs perturbations.

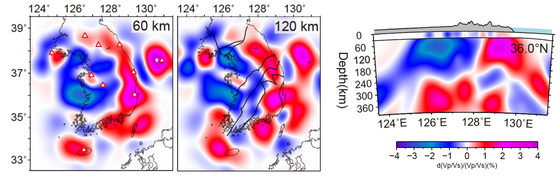

Resolution tests

The resolution of the velocity model was meticulously assessed by performing multiple synthetic recovery tests. All synthetic data were generated using an identical source-receiver combination as the actual data with Gaussian random noise, whose standard deviation was equivalent to the estimated residual uncertainties. First, we conducted conventional checkerboard tests using various scales (bottom left, ~60 km (Fig. a) and ~120 km (Fig. b)). Second, a spike test was performed using discrete short-wavelength anomalies to better verify the effects due to smearing (bottom right, Fig a). Lastly, we tested the resolution with realistic structural input models, which applied simplified block anomalies to evaluate the vertical resolutions of the interfaces (bottom right, Fig. b). The original shape of the input structures was well-recovered. We interpret the resulting velocity anomalies in the following section for the areas showing robust and reliable recovery in the resolution tests.

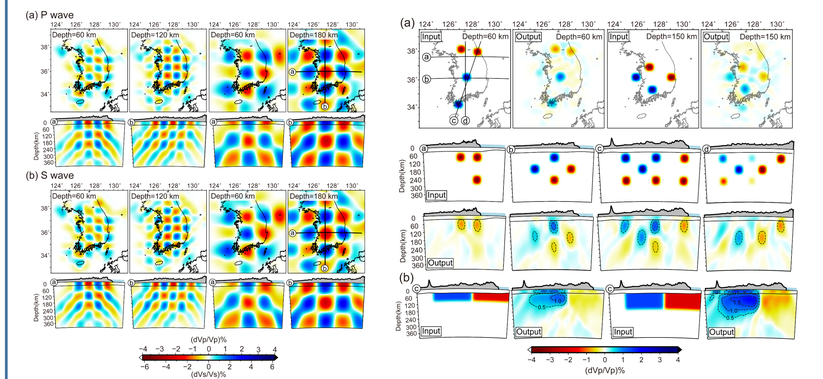

Model regularization

Optimum values of regularization factors (damping (ε) and smoothing (η)) for the model were systematically determined by evaluating the trade-offs between the data misfit, model smoothness, and model variance (Rawlinson et al., 2006)

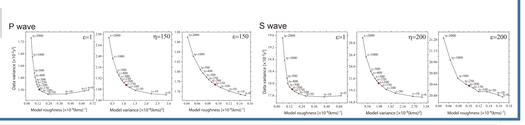

Interpretations

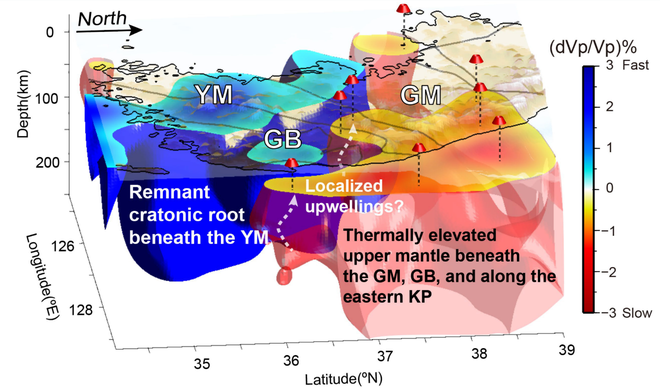

From the global tomography, upper mantle velocity beneath KP exhibits relatively slower than the normal mantle (~-1% of dVp and dVs). Similar velocity patterns were observed in previous regional scale upper mantle tomographic studies in northeast Asia (e.g., Kim et al., 2016; Tao et al., 2018), which were interpreted as velocity contrast between continental lithosphere and asthenosphere (Kim et al., 2016). Based on our results and previous geological and geophysical evidences, the observed velocity pattern is attributable to thickness changes of lithosphere and convective upper mantle. An anomalously thick high-velocity structure beneath the YM suggests the presence of a cold, resistant cratonic lithosphere fragment at the eastern margin of the Eurasian plate. In contrast, the absence of deeper lithosphere mostly occupied by high-temperature, buoyant upper mantle beneath the GM, continental arc and back-arc system of the GB in the southeast, and along the eastern margin indicate highly modified regions. Distinct lithospheric features of the different adjacent Precambrian massifs indicate different responses of each lithosphere to recent marginal tectonic processes. A clear spatial coincidence between low velocities and recent tectono-magmatic activity suggests persistent reactivation of a cratonic margin by intensive interaction between the prominent lithospheric structures and convective upper mantle.

References

Aki, K., Christoffersson, A., Husebye, E.S., 1977. Determination of the three-dimensional seismic structure of the lithosphere. Journal of Geophysical Research 82(2), 277–296.
Chough, S. K., Kwon, S. T., Ree, J. H., Choi, D. K., 2000. Tectonic and sedimentary evolution of the Korean Peninsula: A review and new view. Earth-Science Reviews, 52(1–3), 175–235.
Kim, S., Tkalčić, H., Rhie, J., Chen, Y., 2016. Intraplate volcanism controlled by back-arc and continental structures in NE Asia inferred from transdimensional Bayesian ambient noise tomography. Geophysical Research Letters, 43, 8390–8398.
Laske, G., Masters, G., Ma, Z., Pasyanos, M., 2013, April. Update on CRUST1.0—A 1-degree global model of Earth's crust. In: Geophysical Research Abstract 15, 2658. Vienna, Austria: EGU General Assembly.
Li, C., van der Hilst, R.D., 2010. Structure of the upper mantle and transition zone beneath Southeast Asia from travel time tomography. Journal of Geophysical Research - Solid Earth 115, B07308.
Rawlinson, N., Kennett, B. L. N., 2004. Rapid estimation of relative and absolute delay times across a network by adaptive stacking. Geophysical Journal International, 157(1), 332-340.
Rawlinson, N., Reading, A.M., Kennett, B.L.N., 2006. Lithospheric structure of Tasmania from a novel form of teleseismic tomography. Journal of Geophysical Research 111, B02301.
Rawlinson, N., Sambridge, M., 2004. Wave front evolution in strongly heterogeneous layered media using the fast marching method. Geophysical Journal International, 156(3), 631–647.
Rawlinson, N., Urvoy, M., 2006. Simultaneous inversion of active and passive source datasets for 3-D seismic structure with application to Tasmania. Geophysical Research Letters, 33(24), L24313.
Schmandt, B., Humphreys, E., 2010. Seismic heterogeneity and small-scale convection in the southern California upper mantle. Geochemistry, Geophysics, Geosystems, 11(5).
Song, J. H., Kim, S., Rhie, J., Lee, S. H., Kim, Y., Kang, T. S., 2018. Imaging of lithospheric structure beneath Jeju Volcanic Island by teleseismic traveltime tomography. Journal of Geophysical Research: Solid Earth, 123(8), 6784-6801.
Tao, K., Grand, S. P., Niu, F., 2018. Seismic structure of the upper mantle beneath Eastern Asia from full waveform seismic tomography. Geochemistry, Geophysics, Geosystems, 19(8), 2732-2763.

Acknowledgement

J. S. and J. R. were funded by the Korea Meteorological Institute (KMI) under Grant KMI2019-00110. S. K. was funded by the KMI under Grant KMI2017-01010.